Effect of alkaline earth and transition metals doping on the properties and crystalline perfection of potassium hydrogen phthalate (KHP) crystals†

G. Bhagavannarayana,[a] Shanmugasundaram Parthiban,[b] Chinnusamy Chandrasekaran[b] and Subbiah Meenakshisundaram*[b]

Received 3rd March 2009, Accepted 25th March 2009
First published as an Advance Article on the web 23rd April 2009
DOI: 10.1039/b904220b

The influence of alkaline earth metal (Mg) and transition metal (Hg) doping on the properties and crystalline perfection of potassium hydrogen phthalate (KHP) crystals has been described. Incorporation of dopant into the crystalline matrix even at the low concentrations was well confirmed by energy dispersive X-ray spectroscopy (EDS). Further, high-resolution X-ray diffraction (HRXRD) studies indicate predominant substitutional site occupancy for Mg. Heavy doping results in internal structural grain boundaries due to stress aroused in the lattice caused by the entry of dopants into the crystalline matrix. The transition metal (Hg) doping results in multi-peaks in the diffraction curve (DC) with a wide angular spread and the site occupancy seems to be predominantly interstitial positions in the crystal lattice, quite likely due to its bigger size in comparison with alkaline earth metal. The reduction in the intensity observed in powder X-ray diffraction (XRD) for both types of doped specimens and slight shifts in vibrational frequencies reveal minor structural variations. It is observed that the doping with high concentrations of metal facilitates nonlinearity and enhances the second harmonic generation (SHG) efficiency to a significant extent.

1. Introduction

Potassium hydrogen phthalate (KHP) crystal is well known for its application in the production of crystal analyzers for long wave X-ray spectrometers.[1,2] KHP possesses piezoelectric, pyroelectric, elastic and nonlinear optical (NLO) properties.[3–5] It crystallizes in an orthorhombic structure with space group $Pca2_1$.[6] It has platelet morphology with perfect cleavages along the (010) plane. Using the periodic bond chain analysis, the morphology of potassium hydrogen phthalate has been determined.[7] Recently, KHP crystals have been used as substrates for the growth of highly oriented films of conjugated polymers with nonlinear optical susceptibility.[8,9] KHP is chosen as the model compound because of its well-developed surface pattern on the (010) face consisting of high and very low growth steps which can be relatively easily observed by means of optical microscopy.[10,11] It is used as a substrate for the deposition of thin films of NLO materials, like urea, with high mechanical stability.[12] The Fe/Ce impurity effect on KHP has been studied in detail.[13] Influence of various kinds of impurities on spiral growth phenomena on (010) KHP indicates the existence of different mechanisms of interaction.[14,15] Hottenhuis *et al.*,[16] have made detailed investigations on the surface morphology and the growth kinetics of the KHP (010) face.

Ultraviolet one-color photo refraction (UV-OPR) is enhanced by Mg doping.[17] The second harmonic generation (SHG) conversion efficiency was enhanced by the presence of Mg in $LiNbO_3$ crystals. The optical damage, which is a serious problem with $LiNbO_3$ crystals, can be reduced by doping with Mg.[18] Incorporation of Mg into pure α-$LiIO_3$ crystals significantly enhances the electrical conductivity and the dielectric properties.[19] The substitution of Mg^{2+} ions on the tetrahedral sites in the W-type hexagonal ferrite structure could enhance the magnetic properties.[20] The Mg concentration in Mg-doped $(Ba_{0.6}Sr_{0.4})_{0.92}K_{0.075}TiO_3$ thin films has a strong influence on the materials' properties including surface morphology, dielectric and tunable properties.[21] These aspects prompted us to use Mg as a dopant material in the technologically important KHP crystals. Apart from the general advantages, no studies for Hg as a dopant are available in the literature.

Recently, we have investigated the influence of EDTA doping on the SHG efficiency and crystalline perfection of tris(thiourea)-zinc(II) sulfate (ZTS) crystals.[22] The accommodating capability of ammonium dihydrogen phosphate (ADP) crystals with dopants like KCl and oxalic is an interesting feature.[23] Influence of Mn(II) on the NLO properties of ZTS reveals a good correlation between SHG efficiency and crystalline perfection.[24] As a continuation of our studies to ascertain the influence of doping on the properties and crystalline perfection on some technologically important crystals, this work was undertaken. The literature reveals that doping studies were mostly carried out with dopants with similar atomic/ionic radii as their host crystals. In the present investigation, we have used both light metals of a much smaller size and heavy transition metals for doping and

[a]*Materials Characterization Division, National Physical Laboratory, New Delhi, 110 012, India*
[b]*Department of Chemistry, Annamalai University, Annamalainagar, Tamil Nadu, 608 002, India. E-mail: meenapar@gmail.com; Tel: +91 (0)4144 221670; +91 (0)9443 091274*

† Electronic supplementary information (ESI) available: Powder diffraction data for pure, low and heavy Mg(II) doped KHP and low Hg(II) doped KHP; cell parameter values for low Hg(II) doped KHP; cell parameter values for heavy Mg(II) doping. See DOI: 10.1039/b904220b

the effects on properties and perfection of crystals are systematically analyzed. It has been reported that in the case of calcium tartrate single crystals[25] the doping atom prefers substitution sites when alkaline earth atoms are used, whereas interstitial sites are occupied when a transition metal is used. Also, the cations with radii close to that of Ti^{4+} can substitute for Ti^{4+} in titania crystals, while the cations with large radii, such as Nd^{3+}, Ag^{+}, La^{3+}, Ni^{2+}, Y^{3+} and Rb^{+}, occupy interstitial sites in anatase crystals.[26] HRXRD studies in the present investigation also confirmed this behavior. In the present investigations, the doping of the alkaline earth and transition metals was carried out intentionally to study the effect of size on the accommodation capability of the KHP crystal, dependence of the nature of the additives on properties and their impact on the crystalline perfection which may in turn influence the physical properties, like SHG *etc.*

2. Experimental

Synthesis and crystal growth

KHP (E-Merck) was purified by repeated recrystallization. The crystals were grown by a slow evaporation solution growth technique (SEST). A saturated aqueous solution of KHP was prepared (12 g per 100 ml). Mg(II) in the form of $MgCl_2$ (SDS) and Hg(II) in the form of $HgCl_2$ (BDH) were used. Different concentrations of Mg [1 mol%, (low, l), 20 mol% (heavy, h)] and low concentrations of Hg [1 mol%, (low, l)] were introduced into the aqueous growth medium as dopants. The seed crystals are allowed to float on the surface of the saturated solution and left for slow evaporation at room temperature (30 °C). Triply distilled water was used as solvent. The prepared solution was filtered with a micro filter. The crystallization took place within 15–20 days and the crystals were harvested when they attained an optimal size and shape. It is observed visually that the growth rate of crystals is high with low concentration of dopants. Quite likely, at high concentrations of the dopant, the adsorption film blocks the growth surface and inhibits the growth process.[22,27] Bulk crystals are grown using optimized growth parameters. High quality transparent crystals were harvested from the growth medium at low concentrations of dopants. Photographs of the as-grown doped and undoped crystals are shown in Fig. 1.

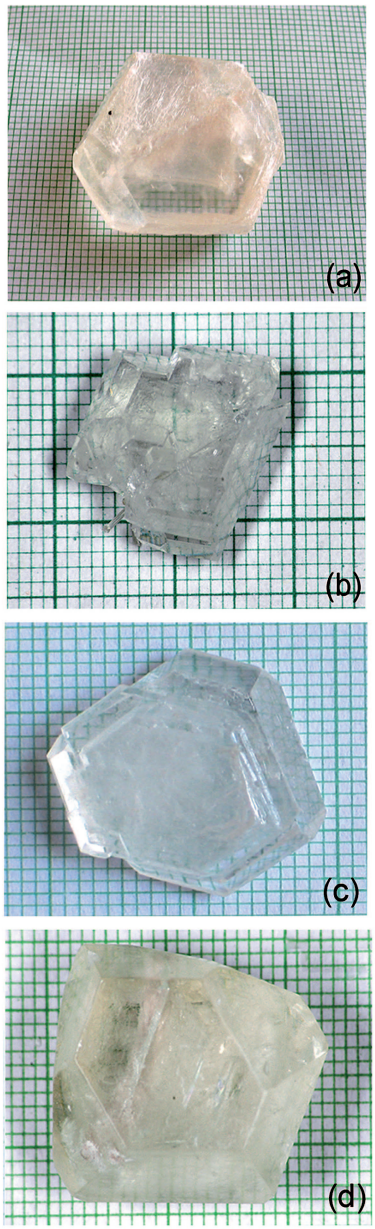

Fig. 1 Photographs of KHP as-grown crystals: (a) Pure, (b) 1 mol% $MgCl_2$ doped, (c) 20 mol% $MgCl_2$ doped and (d) 1 mol% $HgCl_2$ doped.

Characterization techniques

The Fourier transform infrared (FT-IR) spectra were recorded using AVATAR 330 FT-IR by the KBr pellet technique. A Bruker AXS (Kappa Apex II) X-ray diffractometer was used for single crystal X-ray diffraction (XRD) studies. The powder X-ray diffraction was performed by using a Philips Xpert Pro Triple-axis X-ray diffractometer at room temperature using a wavelength of 1.540 Å and a step size of 0.008°. The samples were examined with Cu Kα radiation in a 2θ range of 10 to 70°. The XRD data were analyzed by the Rietveld method with RIETAN–2000.[28] The incorporated magnesium and mercury content in the specimens were analyzed by a Philips Atomic Absorption spectrometer. Morphologies of the samples and the presence of dopants in the specimens were observed by using a JEOL JSM 5610 LV scanning electron microscope with a resolution of 3.0 nm, an accelerating voltage of 20 kV and maximum magnification of 300 000 times. The standards used to study EDS were MgO and HgTe for Mg and Hg dopants respectively.

The SHG test on the crystals was performed by the Kurtz powder method.[29] An Nd:YAG laser with a modulated radiation of 1064 nm was used as the optical source and directed on the powdered sample through a filter. The grown crystals were ground to a uniform particle size of 125–150 μm and then packed in a micro capillary of uniform bore and exposed to laser radiation. The output from the sample was monochromated to collect the intensity of the 532 nm component and to eliminate the fundamental.

To reveal the crystalline perfection of the grown crystals and to study the effect of dopants added in the saturated aqueous solution during the growth process, a multicrystal X-ray

diffractometer (MCD) developed at the National Physical Laboratory[30] was used to record high-resolution rocking or diffraction curves (DC). In this system a fine focus (0.4 × 8 mm; 2 kW Mo) X-ray source energized by a well-stabilized Philips X-ray generator (PW 1743) was employed. The well-collimated and monochromated Mo $K\alpha_1$ beam obtained from the three monochromator Si crystals set in a dispersive (+, −, −) configuration was used as the exploring X-ray beam. This arrangement improved the spectral purity ($\Delta\lambda/\lambda < 10^{-6}$) of the Mo $K\alpha_1$ beam. The divergence of the exploring beam in the horizontal plane (plane of diffraction) was estimated to be $\ll 3$ arc s. The specimen crystal was aligned in the (+, −, −, +) configuration. Although the lattice constant of the monochromator crystal(s) and the specimen were different, due to the dispersive configuration, the unwanted dispersion broadening in the DC of the specimen crystal was insignificant. The specimen could be rotated about a vertical axis, which was perpendicular to the plane of diffraction, with a minimum angular interval of 0.5 arc s. The diffracted intensity was measured by using a scintillation counter. The DCs were recorded by changing the glancing angle (angle between the incident X-ray beam and the surface of the specimen) around the Bragg diffraction peak position θ_B (zero taken as reference point), starting from a suitable arbitrary glancing angle (θ). The detector was kept at the same angular position $2\theta_B$ with a wide opening for its slit, the so-called ω scan. For all the specimens in the present study, the X-ray power, size of the beam and configuration of the diffractometer were kept constant. Before recording the DCs, to remove the non-crystallized solute atoms remaining on the surface of the crystal and also to ensure the surface planarity, the specimens were first lapped and chemically etched in a non-preferential etchant of water and acetone mixture in a 1 : 2 volume ratio.

3. Results and discussion

FT-IR analysis

A very slight shift in some of the characteristic vibrational frequencies of pure KHP is observed because of doping with Mg/Hg. It could be due to the lattice strain developed as a result of doping.

SEM and EDS

The effect of the influence of dopants on the surface morphology of KHP crystal faces revealed some interesting features. Plate morphology was observed for the undoped KHP; the highest surface roughness could be due to bunched steps or macrosteps. The Hg-doped crystal has the lowest surface corrugation. The earlier studies[31] on doped KHP crystals indicate that the dopants lead to mosaicity. The addition of 16 ppm Ce^{3+} ions on the KHP shows that the steps were retarded and bunching occurred.[14] Interestingly, by the addition of 16 ppm Fe^{3+} under identical growth conditions the opposite effect was observed. Instead of lengthening, the growth spirals shortened along their *c*-direction.[14] It is clear from the investigations that the doping changes the morphology, resulting in crystal voids.

The presence of Mg in the doped specimen was confirmed by EDS (Fig. 2) and a higher concentration of Mg dopant led to increased incorporation of Mg into the crystalline matrix.

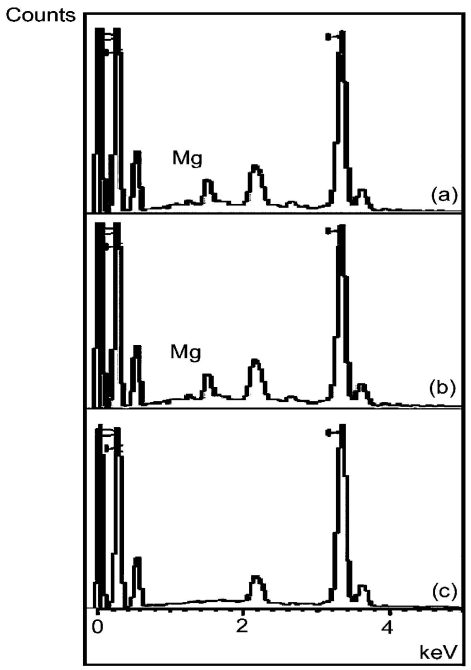

Fig. 2 EDS of KHP crystals: (a) 1 mol% $MgCl_2$ doped, (b) 20 mol% $MgCl_2$ doped and (c) 1 mol% $HgCl_2$ doped.

Analysis of the surface at different sites reveals that the incorporation is non-uniform over the surface, and connected with the absorption mechanisms at the ledges of step strains. Interestingly, Hg is not observed in the EDS spectrum (Fig. 2). It might be segregated along the internal structural boundaries as evidenced by HRXRD studies. Inner parts of the doped crystals are exposed by cleaving along the (010) plane for measuring subsurface element concentrations (Fig. 3) and the EDS for cleaved crystals clearly identifies Hg (Fig. 3). However, EDS is a poor technique for quantitative analysis.

Atomic absorption spectroscopy (AAS)

This technique was used to quantify the concentration of the dopant present in KHP crystals using a graphite line as internal standard. The data reveals that the dopant concentrations incorporated into the KHP lattices were 9.16 (1 mol% Mg), 12.67 (20 mol% Mg) and 0.09 (1 mol% Hg) ppm. It is clear that the accommodation of the dopant into KHP crystalline matrix is not proportional to the amount of dopant used in the crystallization process. The quantity of foreign metal ions entering into the crystalline matrix is much less in comparison with the quantity introduced into the aqueous growth medium. It could be due to the limitations of the accommodating capability of the material. The main reason for the lower accommodating capability of KHP crystals for Hg dopant than for Mg obviously seems to be due to the latter's larger size.

UV-Vis spectral studies

The UV spectrum reveals that the cut off wavelength is ~300 nm. Absorption is minimum in the 300–1100 nm region. It appears that the doping does not destroy the optical transmission. No

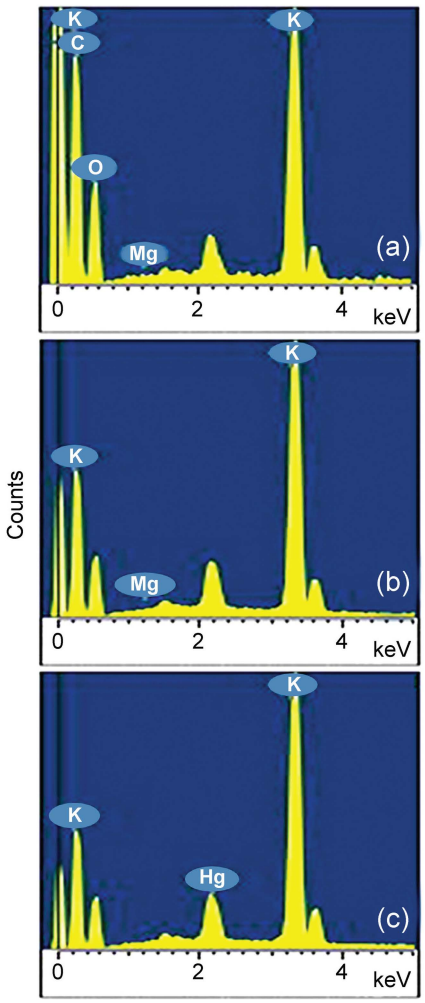

Fig. 3 EDS of inner part of KHP crystals: (a) 1 mol% $MgCl_2$ doped, (b) 20 mol% $MgCl_2$ doped and (c) 1 mol% $HgCl_2$ doped.

significant λ_{max} shift is observed but the absorbance is reduced drastically by doping. Because of high transparency, these doped crystals are quite useful for optical device applications.

SHG efficiency

An SHG test was performed on the powder samples with an input radiation of 2.5 mJ $pulse^{-1}$. The output SHG intensities (Table 1) for pure and doped specimens give relative NLO efficiencies of the measured specimens. Significant enhancement of SHG efficiency is reached with a high dopant concentration and it was also observed that the SHG efficiency is concentration (of the dopant) dependent.

Table 1 SHG outputs

System	$I_{2\omega}$/mV
Pure KHP	27–29
Mg-doped KHP (l)	30–32
Mg-doped KHP (h)	52–53
Hg-doped KHP (l)	32–34

The depressed SHG efficiency is quite likely due to the disturbance of charge transfer. An efficient SHG demands a specific molecular alignment of the crystal to be achieved, facilitating nonlinearity in the presence of a dopant. It has been reported that the SHG can be greatly enhanced by attaining the molecular alignment through inclusion complexation.[32] Recently, we have reported that the enhancement in crystalline perfection could lead to an improvement in SHG efficiency.[31]

XRD and HRXRD

The lattice constants for heavily Mg-doped KHP (h) obtained by cell refinement with least square fitting of the lines in the range of $20° \leq 2\theta \leq 120°$ are $a = 9.6329$ (± 0.0144); $b = 13.3035$ (± 0.0299); $c = 6.4786$ Å (± 0.0084); $V = 830.1192$ $Å^3$ (± 2.4834). The corresponding values for 1 mol% Hg-doped KHP (l) are $a = 9.62$ (± 0.06); $b = 13.33$ (± 0.08); $c = 6.48$ Å (± 0.04) and $V = 832$ $Å^3$ (± 3). The JCPDS (00–031–1855) values for pure KHP are $a = 9.6120$; $b = 13.3290$; $c = 6.4820$ Å and $V = 830.46$ $Å^3$. The powder XRD patterns of doped KHP samples are compared with that of the undoped one (Fig. 4). Quantitative data shows slight changes in the lattice parameter values and hence the unit cell volume. The radius of the dopants, Mg^{2+} (72 pm) and Hg^{2+} (83 pm) are very small compared with that of K^+ (151 pm).[33] Hence, it is reasonable to believe that the dopant can enter into the KHP crystalline matrix without causing much distortion.

The partial substitution of K^+ by Mg^{2+}/Hg^{2+} leads to the formation of cation vacancies to preserve electrical neutrality. An analogous type of defect center with cation vacancy formation is well established in the study of Mn(II)-doped KDP (potassium dihydrogen phosphate) crystals[34] by computer structural modelling. It appears that there is no change in the basic structure of the XRD patterns. No new peaks or phases were observed by doping with alkaline earth and transition

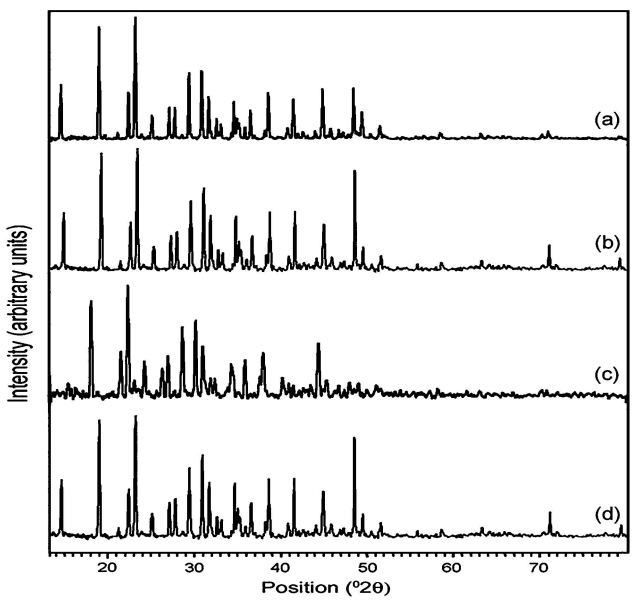

Fig. 4 Powder X-ray diffraction curves of KHP crystals: (a) pure, (b) 1 mol% $MgCl_2$ doped, (c) 20 mol% $MgCl_2$ doped and (d) 1 mol% $HgCl_2$ doped.

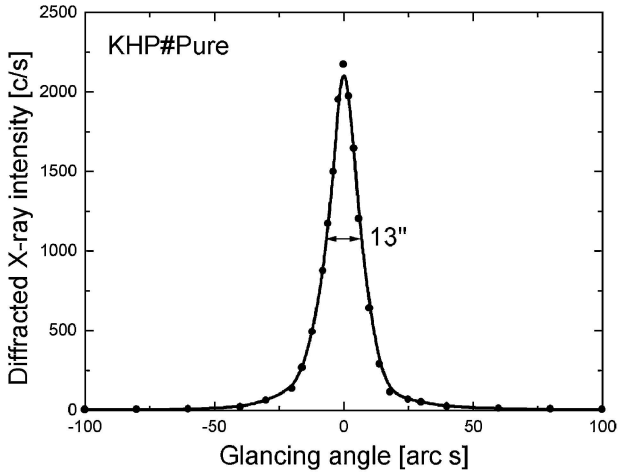

Fig. 5 High-resolution X-ray diffraction curve (DC) recorded in a symmetrical Bragg geometry for an undoped KHP crystal specimen using (010) planes.

metals. However, a considerable reduction in intensity is observed because of doping. The slight structural changes indicate the lattice strain due to the doping. The crystallite size of crystalline domains which diffract coherently is decreased from ~48 nm (for pure KHP) to ~26 and ~43 nm for the light metal magnesium and transition metal mercury respectively.

Fig. 5 shows the high-resolution X-ray diffraction curve for the undoped KHP crystal recorded for the (010) diffracting planes using Mo $K\alpha_1$ radiation in a symmetrical Bragg geometry. The curve is quite sharp having full width at half maximum (FWHM) of 13 arc s with a good symmetry with respect to the exact diffraction peak position (taken as zero), as expected for a nearly perfect crystal according to the plane wave dynamical theory of X-ray diffraction.[35]

Fig. 6 shows the DCs for the 1 mol% doped KHP single crystals recorded under identical conditions as that of Fig. 5 for the undoped specimen. The DC of curve (a) was recorded with a simple washing after it is harvested from the solution. As seen in the Fig., the curve does not contain any additional peaks, but

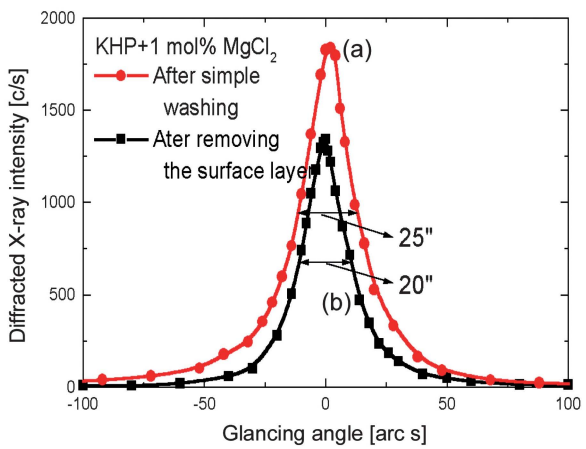

Fig. 6 DCs recorded under similar conditions as that of Fig. 5 for 1 mol% $MgCl_2$ doped KHP crystals: (a) recorded with simple washing and (b) recorded after removal of surface layer.

it is significantly broader than the DC of Fig. 5, having an FWHM of 25 arc s. The intensity along the wings of the curve on both sides of the diffraction peak position is also very high. One may notice that the intensity at angular distances of up to 100 arc s on both sides of the exact Bragg peak position (denoted as zero) do not decrease to zero, which is otherwise expected to be nearly zero for any reasonably good quality crystal even though its FWHM may be of the same order (*i.e.* around 25 arc s). The broadness of the DC indicates that the quality of the specimen crystal is slightly decreased due to doping.

The combined features of the symmetry of the curve with respect to the exact peak position and the increase in FWHM value indicates some mosaic nature of the crystal. The mosaic blocks seem to be oriented randomly, with their normals misoriented with respect to each other by an angle of a few arc s. It is interesting to compare this feature with the similar feature observed in our earlier study on KHP doped with 1,10-phenanthroline (phen).[31] To confirm whether this mosaic nature is limited to the surface due to the complexing layer formed by the dopants in the solution with Mg dopant, the surface was lapped to remove a few microns of surface and then chemically etched with a mixture of acetone and water in a 1 : 2 volume ratio. Curve (b) in the Fig. shows the DC obtained after removing the surface layer. The FWHM is reduced to 20 arc s from the initial value of 25 arc s. This reduction, though significant, is not to the same extent as that observed in the case of phen dopant. This could be mainly due to the fact that the phen dopant concentration used in those studies[31] was too small (0.01 mol%). Furthermore, due to its large size, no significant quantity of dopant could have entered into the crystalline lattice. In the present case of Mg, due to the comparatively high concentration, significant amounts of Mg dopant might have entered into the lattice which might be the reason for the increase in the FWHM value even in the bulk crystal. The symmetry in the DC (Fig. 6) also indicates that most of the dopants occupy the substitutional positions. As observed in our recent investigation[23] on KCl and oxalic acid doped ADP crystals, if the dopant occupies interstitial positions, asymmetry in the DC is expected, with more intensity on the higher diffraction angle with respect to the exact peak position. It is also interesting to compare the integrated intensities (*i.e.* the area under the DC, normally denoted by ρ) of the curves of Fig. 6. It is shown that the bulk crystal has relatively better crystalline perfection than that of the surface layer since the integrated intensity of the surface layer is reduced to around 35% of the integrated intensity bulk. It may be mentioned here that $\rho \propto F^2_{hkl}$ (F_{hkl} being the structure factor) in the case of an ideal mosaic crystal and $\rho \propto F_{hkl}$ for an ideal perfect crystal[36] and hence $\rho_{mosaic} > \rho_{perfect}$.

Fig. 7 shows the DC recorded for a typical KHP specimen crystal doped with 20 mol% $MgCl_2$ using (010) diffracting planes under the same experimental conditions as that of Fig. 5 and 6. In contrast to Fig. 5 and 6, this DC contains one well resolved additional peak and another less prominent peak merged with the main peak. The solid line (convoluted curve) is well fitted with the experimental points represented by the filled rectangles. On deconvolution of the diffraction curve using Lorentzian curve fitting, it is clear that the curve contains two additional peaks, which are 753 and 60 arc s away from the main peak. These two additional peaks correspond to two internal structural

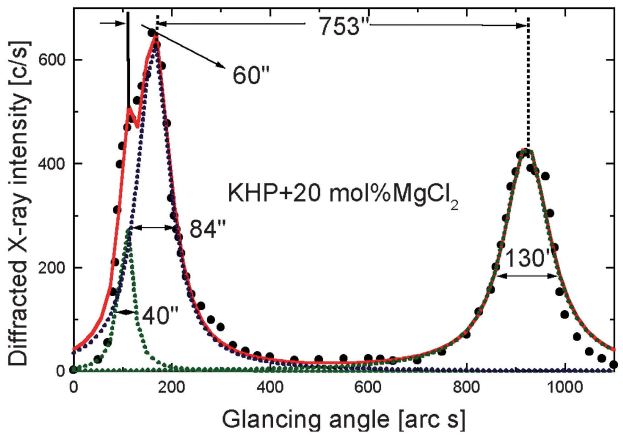

Fig. 7 High-resolution X-ray diffraction curve (DC) recorded in a symmetrical Bragg geometry for a typical 20 mol% $MgCl_2$ doped KHP single crystal specimen using (010) planes.

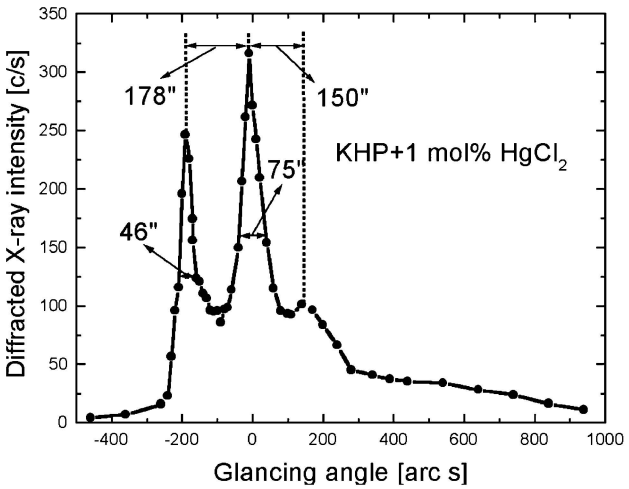

Fig. 8 DCs recorded for typical KHP crystals using (010) diffracting planes with 1 mol% doping of $HgCl_2$.

low angle (tilt angle ≥ 1 arc min but less than a degree) boundaries[37] whose tilt angles (misorientation angle between the two crystalline regions on both sides of the structural grain boundary) are 753 and 60 arc s from their adjoining regions.

The FWHM of the main peak and the low angle boundaries are 84, 130 and 40 arc s, respectively. Though the specimen contains low angle boundaries, the relatively low angular spread of around 17 arc min of the diffraction curve and the low FWHM values show that the crystalline perfection is reasonably good. The effect of such low angle boundaries may not be very significant in many applications, but for the phase matching applications, it is better to know these minute details regarding crystalline perfection. However, if we compare the crystalline perfection of this specimen with that of pure and 1 mol% doped crystals, its perfection is very low. These results clearly indicate that at higher concentrations, the crystal develops internal structural boundaries due to heavy stress in the lattice caused by the entry of an extra amount of dopants at the interstitial positions, in addition to the balanced occupation of dopants at the substitutional sites. It has been established in our study of tris-(thiourea)copper(I) chloride crystals that the replacement of Cu(I) by Co(II) leads to the formation of cation vacancies to maintain electrical neutrality.[38] Such vacancies cause tensile strain in the lattice and broadening of diffraction peaks. Substantial peak broadening due to doping is observed in the DCs of HRXRD in the present investigation and it provides evidence for the stress development in the host crystal due to doping.

Fig. 8 shows the DC recorded for KHP crystals doped with Hg, using (010) diffracting planes in a symmetrical Bragg geometry under the same experimental conditions as that of Fig. 5.

As seen in the Fig., the DC contains multi-peaks with a wide angular spread of around 25 arc min which is nearly half a degree of arc, showing that the crystalline quality is not good enough. However, the sharp peaks for the individual boundaries with FWHM values of 46 and 75 arc s indicate that the crystalline perfection of individual grains is not that bad. It may be mentioned here that though the crystal contains grain boundaries, on both sides of the boundary the crystalline regions or the grains may be perfect parts of the crystal and such parts or grains may be misoriented by a definite angle which can be quantitatively obtained by measuring the angle between the adjacent peaks of the DC. It seems, due to the larger size of the host crystal than that of the metal ion, these dopants could not take the substitutional positions, but entered into the interstitial sites of the crystalline matrix during the growth process. However, due to internal stress aroused in the crystal by the dopants, the crystal develops structural grain boundaries and the dopants segregate along the boundaries by the process of guttering as observed in oxalic acid doped ADP crystals.[23] The DC has an asymmetry with respect to the peak position, with more scattered intensity on the higher glancing angle side than that on the lower glancing angle side for a particular deviation angle ($\Delta\theta$) from the zero position, and indicates that the metal takes the interstitial positions. These results indicate that the transition metal predominantly occupies the interstitial positions, whereas alkaline earth metals occupy the substitutional positions. However, there is a limit on the amount of dopant which can be accommodated by the crystal depending upon the size of the dopant. At higher doping levels, even in the light alkaline earth metals, a good amount of dopants also occupy the interstitial positions which may finally lead to generation of grain boundaries and along the boundaries these interstitially entered dopants seem to segregate just like Si impurities segregated in bismuth germinate, $Bi_4Ge_3O_{12}$ crystals at the boundaries in our earlier studies.[39]

4. Conclusions

We have used XRD, FT-IR, SEM, EDS, HRXRD, UV-Vis and Kurtz powder techniques to study the influence of doping with a light alkaline earth metal (Mg) and a heavy transition metal (Hg) on KHP crystals. A close observation of XRD profiles of doped and undoped samples reveals some minor structural variations due to lattice stress as a result of doping. The HRXRD investigations show that Mg at moderate doping levels occupies predominantly substitutional positions because of its comparatively smaller ionic radius while the heavy transition metal mainly occupies the interstitial sites. However, at higher doping levels, a good amount of lighter dopant like Mg also enters into

the interstitial positions, resulting in structural grain boundaries which are responsible for the observed additional peaks in high-resolution diffraction curves. The general conclusion from this investigation is that a significant enhancement of SHG efficiency can be reached with a high dopant concentration.

Acknowledgements

One of the authors, GB, acknowledges Dr Vikram Kumar, Director, NPL and Dr B.R. Chakraborthi for their constant encouragement to carry out the present investigations. The authors are grateful to the authorities of Annamalai University for providing various experimental facilities used in the present investigation.

References

1 J. L. Jones, K. W. Paschen and J. B. Nicholson, *Appl. Opt.*, 1963, **2**, 955 961.
2 O. Yoda, A. Miyashita, K. Murakami, S. Aoki and N. Yamaguchi, *Proc. SPIE-Int. Soc. Opt. Eng.*, 1991, **1503**, 463 466.
3 A. Miniewicz and S. Bartkiewicz, *Adv. Mater. Opt. Electron.*, 1993, **2**, 157 163.
4 N. Kejalakshmy and K. Srinivasan, *Opt. Mater.*, 2004, **27**, 389 394.
5 M. V. Shankar and K. B. R. Varma, *Ferroelectr., Lett. Sect.*, 1996, **21**, 55 59.
6 Y. Okaya, *Acta Crytallogr.*, 1965, **19**, 879 882.
7 M. H. J. Hottenhuis, J. G. E. Gardeniers, L. A. M. J. Jeti'en and P. Bennema, *J. Cryst. Growth*, 1988, **92**, 171 188.
8 M. Nisoli, V. Pruneri, V. Magni, S. De Silvestri, G. Dellepiane, D. C. Cuniberti and J. Le Moigne, *Appl. Phys. Lett.*, 1994, **65**, 590 592.
9 S. Timpanaro, A. Sassella, A. Borghesi, W. Porzio, P. Fountaine and M. Goldmann, *Adv. Mater.*, 2001, **13**, 127 130.
10 W. J. P. Van Enckevort and L. A. M. J. Jetten, *J. Cryst. Growth*, 1982, **60**, 275 285.
11 G. R. Ester, R. Price and P. J. Halfpenny, *J. Cryst. Growth*, 1997, **182**, 95 102.
12 P. Murugakoothan, R. Mohankumar, P. M. Ushashree, R. Jayavel, R. Dhansekaran and P. Ramasamy, *J. Cryst. Growth*, 1999, **207**, 325 329.
13 M. H. J. Hottenhuis and A. Oudenampsen, *J. Cryst. Growth*, 1988, **92**, 513 529.
14 M. H. J. Hottenhuis and C. B. Lucasius, *J. Cryst. Growth*, 1986, **78**, 379 386.
15 M. H. J. Hottenhuis and C. B. Lucasius, *J. Cryst. Growth*, 1988, **91**, 623 631.
16 M. H. J. Hottenhuis and C. B. Lucasius, *J. Cryst. Growth*, 1989, **94**, 708 720.
17 H. Qiao, J. Xu, Y. Tomita, D. Zhu, B. Fu, G. Zhang and G. Zhang, *Opt. Mater.*, 2007, **29**, 889 895.
18 T. Zhang, B. Wang, Y. Zhao, S. Fang, D. Ma and Y. Xu, *Mater. Chem. Phys.*, 2004, **88**, 97 101.
19 Y. Du, Y. Sun, W. C. Chen, X. L. Chen and D. F. Zhang, *J. Cryst. Growth*, 2006, **291**, 424 427.
20 M. A. Ahmed, N. Okasha, M. Oaf and R. M. Kershi, *J. Magn. Magn. Mater.*, 2007, **314**, 128 134.
21 M. Nakamura, M. Sekita, S. Takekawa and K. Kitamura, *J. Cryst. Growth*, 2006, **290**, 121 126.
22 S. Meenakshisundaram, S. Parthiban, N. Sarathi, R. Kalavathy and G. Bhagavannarayana, *J. Cryst. Growth*, 2006, **293**, 376 381.
23 G. Bhagavannarayana, S. Parthiban and Subbiah Meenakshisundaram, *Cryst. Growth Des.*, 2007, **8**, 446 451.
24 G. Bhagavannarayana, S. K. Kushwaha, S. Parthiban and Subbiah Meenakshisundaram, *J. Cryst. Growth*, 2009, **311**, 960 965.
25 M. E. Torres, T. López, J. Stockel, X. Solans, M. G. Vallés, E. R. Castellón and C. G. Silgo, *J. Solid State Chem.*, 2002, **163**, 491 497.
26 Z. M. Shi, L. Yan, L. N. Jin, X. M. Lu and G. Zhao, *J. Non-Cryst. Solids*, 2007, **353**, 2171 2178.
27 V. A. Kuznetsov, J. M. Okhrimenko and M. Rak, *J. Cryst. Growth*, 1998, **193**, 164 173.
28 F. Izumi and T. Ikeda, *Mater. Sci. Forum*, 2000, **321–324**, 198 203.
29 S. K. Kurtz and T. T. Perry, *J. Appl. Phys.*, 1968, **39**, 3798 3813.
30 K. Lal and G. Bhagavannarayana, *J. Appl. Crystallogr.*, 1989, **22**, 209 215.
31 G. Bhagavannarayana, S. Parthiban and S. Meenakshisundarm, *J. Appl. Crystallogr.*, 2006, **39**, 784 790.
32 Y. Wang and D. F. Eaton, *Chem. Phys. Lett.*, 1985, **120**, 441 444.
33 R. D. Shannon, *Acta Crystallogr., Sect. A*, 1976, **32**, 751 757.
34 M. Rak, N. N. Eremin, T. A. Eremina, V. A. Kuznetsov, T. M. Okhrimenko, N. G. Furmanova and E. P. Efremova, *J. Cryst. Growth*, 2005, **273**, 577 585.
35 B. W. Batterman and H. Cole, *Rev. Mod. Phys.*, 1964, **36**, 681 717.
36 R. W. James, *The Optical Principles of the Diffraction of X-Rays*, Ox Bow Press, London, 1950, p. 271.
37 G. Bhagavannarayana, R. V. Ananthamurthy, G. C. Budakoti, B. Kumar and K. S. Bartwal, *J. Appl. Crystallogr.*, 2005, **38**, 768 771.
38 G. Bhagavannarayana, S. K. Kushwaha, S. Parthiban, G. Ajitha and Subbiah Meenakshisundaram, *J. Cryst. Growth*, 2008, **310**, 2575 2573.
39 A. Choubey, G. Bhagavannarayana, Y. V. Shubin, B. R. Chakraborty and K. Lal, *Z. Kristallogr.*, 2002, **217**, 515 521.